

An analysis of the influence of microclimate on partial discharge activity in emissions of electric machines in the conditions of industrial operation – own research

ZBIGNIEW PLUTECKI, SŁAWOMIR SZYMANIEC

*Department of Electrical, Control and Computer Engineering
Opole University of Technology, Opole, Poland
e-mail: z.plutecki@po.opole.pl*

(Received: 07.01.2013, revised: 06.09.2013)

Abstract: The article presents the results of diagnostic measurements of partial discharge signal propagation from the winding insulation in electrical machinery, which were performed using an on-line method. This paper describes the results of experiments and the acquired experience in the monitoring of winding insulation in high power and high voltage electrical machines which are important in industrial production processes. The authors show the measurement techniques employed in their research. Representative measurement results are presented along with their analysis. The authors use an *SKF* monitoring systems to measure: vibrations, temperature, and humidity, as major factors affecting partial discharge activity in the from winding insulation of electrical machines.

Key words: HV electrical machines, partial discharge in winding insulation, *on-line* insulation diagnosis, microclimate

1. Introduction

Nowadays, partial discharge measuring methods are becoming the main methods for evaluating the condition of winding insulation in motors and generators. Contemporary measurements of partial discharges (*PDs*) are becoming one of the key points in routine motor testing programs, and they provide a plethora of information of the quality of machine production, as well as of the state of winding insulation in machines. Considering the operational status of the machine two methods of partial discharge measurement can be distinguished: *off-line* (in a standstill), and *on-line* (during the operation) [6, 10, 11, 12, 16]. *PD* generation by insulation, in industrial exploitation conditions, is different than in the *off-line* mode. Motor's operation generates the electro-dynamic forces, especially in the front parts of the windings, which together with the electric stress give rise to *PD*. Insulation of motors in a standstill, during off-line testing, is stressed only by means of high voltage. The intensity of *PD* pulses (count rate, magnitude, frequency range, etc.) is much lower than that measured during the actual exploitation. Deterioration of the condition of winding insulation in various parts of the

system occurs in a different degree and at a different pace. As far as technical means allow, this should be taken into consideration during the motor diagnosis process. In electric machines, *PD* measurements are most often performed on generators, but nowadays, they more and more often include *HV* electrical motors. The requirements of norms, recommendations, certification programs trade data of electronic products of the highest quality that contain data concerning the requirements towards the *PD* level [1, 3, 5, 13, 15-17].

2. The main reasons for the ageing of winding insulation

The lifetime of winding insulation of motors and generators in industrial exploitation conditions depends on many factors. The most important of them are stresses induced by variable thermal, electrical, and mechanical conditions, as well as stresses induced by ambient (environmental) conditions (Fig. 1) [7, 8, 11, 17]. Each of these affects the condition of insulation individually. When they occur collectively however, they form the so-called compound effect. One of the effects of the process of ageing insulation is, for example, delaminating insulation, resulting in voids and bubbles which, when accessed by the air, form, the so-called, gaseous inclusions (Fig. 2) [4].

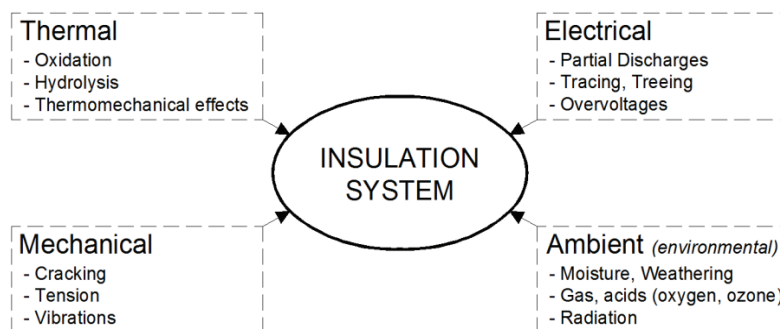


Fig. 1. Ageing stresses (according to IEC 60505) [11]

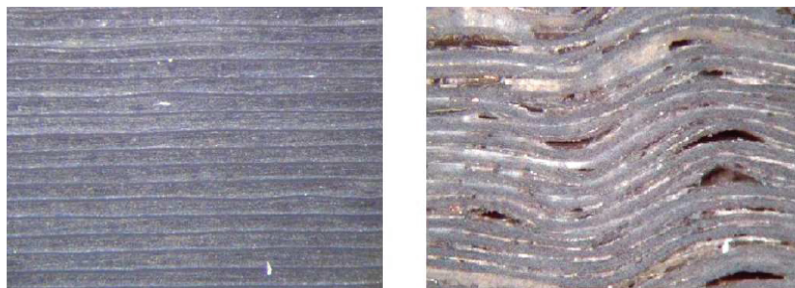


Fig. 2. Mica-based insulation showing perfect (left) and wrinkled tape layers with many voids (right) [4]

Appropriate protection of electrical machinery during industrial exploitation is very important to minimize the rate of breakdowns, preventing breakdowns of accompanying equipment, and ensuring safety of both the personnel and production goals. The document titled “A Report of Large Motoric Reliability Survey of Industrial and Commercial Installations”, published by the *IEEE* and the *EPRI*, lists the main reasons for electrical motor breakdowns. In spite of various methods of evaluation and applied criteria, research points to similar conclusions in regards to the reasons for breakdowns, connected to mechanical and electrical, thermal, and ambient conditions. By analyzing the data supplied by the report, one comes to the conclusion that many of the breakdowns are caused directly or indirectly not only by electrical and chemical, but also by the environmental conditions of the workplace of the machine. The share of the latter conditions is estimated to be 38.7% and 32% [10], respectively. The main reason is a too high or too low of a temperature, humidity of the air, as well as an inappropriate cooling of motor winding, which comprises as much as 12.7% [11]. These state of affairs should be blamed mainly on not appreciating the impact enough of these parameters on the ageing process.

3. The PD activity in winding insulation of HV machinery

The complex structure of insulation materials used in HV induction motors and the specificity of the technological process of their insulation system may be the reason for the occurrence of internal defects – most often in the form of gaseous inclusions, areas of varying dielectric permittivity, needle points on the surface, and so forth. Insulation systems of *HV* motors work under the conditions of multifactor exposure, resulting in the magnification of already existing, and newly forming defects. The ageing process of insulation is accompanied by the occurrence of the phenomenon of *PD*. Partial discharges are discharges occurring inside insulation systems that only partially bridge the insulation between conductors, which do or do not develop at the conductor [2, 6, 10, 12, 14]. They are generally considered to be local discharges in insulation and, in many cases, they occur well in advance of a full breakdown of the insulation [12, 14]. In general terms, *PD* occurs as a result of local electric stress concentration inside the insulation, or on its surface, and it usually takes the form of impulses of duration not exceeding 1 μ s [10]. If the local electric field exceeds certain threshold for the inception of discharge (for example $E \geq 3$ kV/mm [5, 13]) in the presence of the initiating electron, it forms an electron avalanche is formed [14]. The phenomenon is limited in space and is temporary in its character [13, 14]. The impact of this kind of phenomena on the insulation is a gradual deterioration, especially as a result of an accumulation of damage, accompanied by non-expiring *PDs* [6, 13, 14]. It is one of the constituents of the operation related ageing of insulation. As research proves [4, 6, 11, 13, 14], *PDs* are the main symptoms of damaged insulation caused by its ageing. For that reason detection of *PD* in insulation is an important element of the evaluation of its condition.

4. Own research

4.1. Employed research tools

4.1.1. The measurement of partial discharge

In the team of authors, *PD* measurements are conducted by means of two on-line monitoring systems. The first system consists of an *R500* device manufactured by *Vibrocenter*, nine *DRTD-3* sensors coupled with nine *Pt100* thermistors, mounted on the coiling of the motor's stator, one *RFCT* sensor mounted on the neutral wire, one sensor of the temperature of the air, and one relative air humidity sensor mounted near the motor subject in the research. Additionally, the *R500* device is equipped with one noise channel, and two additional channels for the measurement of current intensity and voltage. All of the channels are insulated, they come with circuit-breakers and HF filters. The *R500TM* acquires pulses of frequency between $1 \div 20$ MHz. The block diagram for the measuring unit is presented in Figure 3. For the purposes of control and the acquisition of discharges in a separate neutral wire, the *RFCT* sensor by *Vibrocenter* is used. The choice of sensor is based on the conditions specified by the producer. The sensor's main characteristic is its high sensitivity to *PD* pulses within the range of

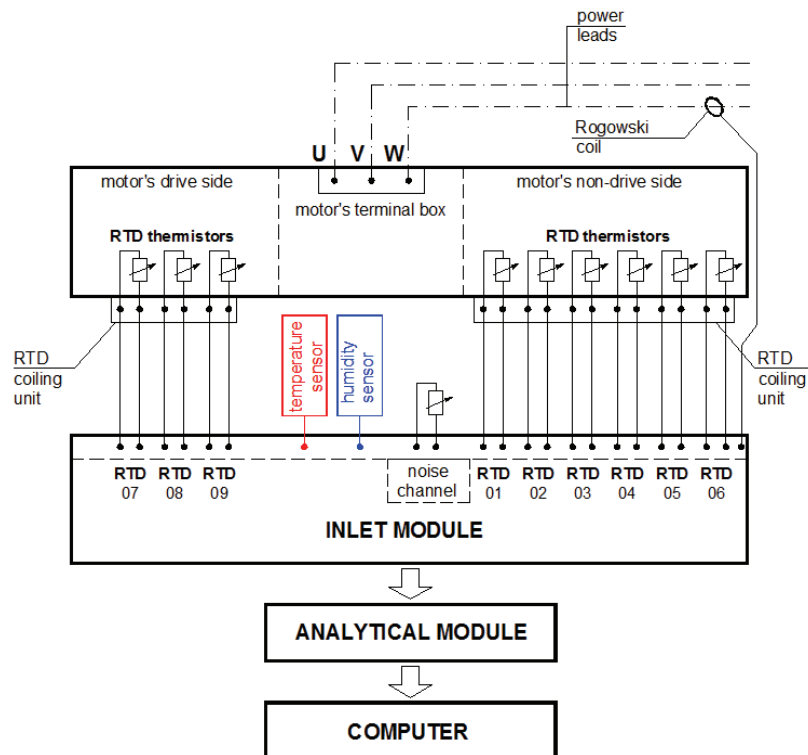


Fig. 3. Simplified block diagram of the measuring unit of a cement mill motor with a rated power of 1 MW, performed with the use of the set for the *PD* measurement of *R500* motors

0.5 MHz – 50 MHz [10]. Part of the research was conducted using a commercial monitoring unit by Eaton. This system includes: an Insulgard measurement device, three 80pF coupling condensers, six RTD sensors coupled with PT thermistors, a temperature sensor, one relative air humidity sensor, a noise channel, and two additional channels for the measurement of current intensity and voltage.

The used measuring units allow for the measurement of the following PD parameters: phase resolved PD patterns, intensity of discharges (PDI), magnitude of discharge (Q_{max}), the number of discharge impulses measured within 1 second (PPS , pulse per second, or pulse count rate).

Thermistors in the measuring system have also the function of radio frequency antennas that acquire partial discharge induced signals and send the signals to the antenna unit DRTD-3. This unit is responsible for the noise suppression and separation of the PD signal from interferences. In the RTD element, the signal is also amplified and relayed over to the unit that monitors partial discharges. DRTD sensors measure the partial discharge signals within the frequency of 1-20 MHz. The example of the location of the nine Pt100 thermistors, placed underneath the wedges inside the slots of the tested motor's stator during its periodic maintenance, has been presented in figure 4.

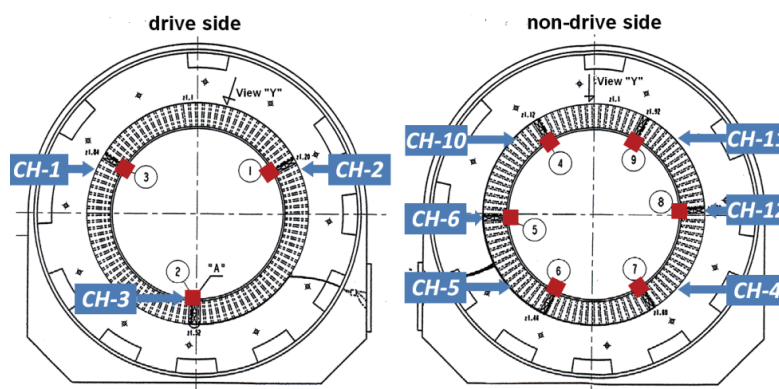


Fig. 4. The situation Pt100 resistors at the drive side (3 pcs.) and the non-drive side (6 pcs.) of the tested motor, and the corresponding measurement channels

The used measuring units allow for the measurement of the following PD parameters: phase resolved PD patterns, intensity of discharges (PDI), magnitude of discharges (Q_{max}), and the number of impulses of discharges measured within 1 second (PPS).

4.1.2. The measurement of mechanical load and auxiliary measurements

The measuring unit consists of an advanced *Multilog IMx-S* analyzer manufactured by *SKF*, whose purpose is to perform continuous diagnosis of the condition of bearings for the purposes of the experiment; and for the purposes of the experiment was expanded by 4 temperature measuring sensors and 4 air humidity sensors placed in the vicinity of the tested motor (Figs. 5-6). The system has 16 dynamic channels (DC) and 8 digital channels. It per-

forms the measurement simultaneously on all of the channels, has the function of generating envelopes and definition of alarm conditions, and the function of buffering data in the internal memory; in the case of a lack of communication, it can be operated by means of @ptitude Observer computer software.

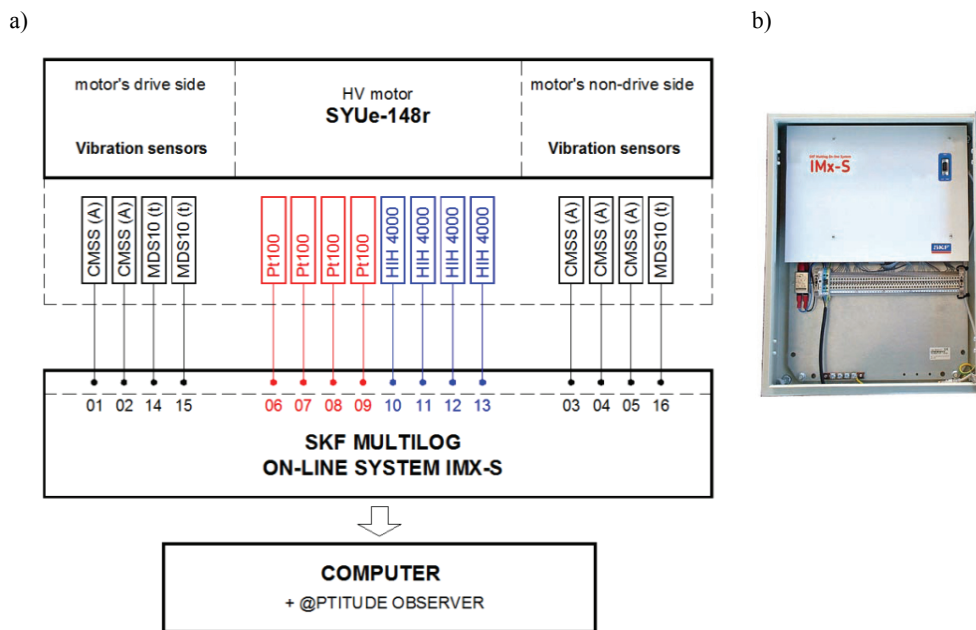


Fig. 5. SKF Multilog on-line system IMx-S: a) block diagram of the measurement unit, Pt100 – temperature measurement, HIH – humidity measurement, CMSS – absolute shock transducers (accelerometers), MDS10 – relative shock transducer (technicad), b) general view

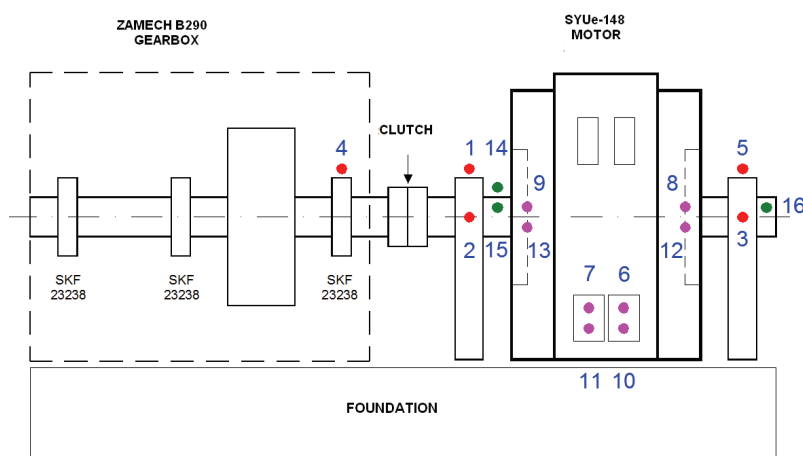


Fig. 6. Block diagram of measurement sensors mounting within the precincts of the tested electrical motor, cooperating with the stationary SKF Multilog IMx-S

The devices employed for the auxiliary measurement are: an *MM-01* microprocessor microclimate meter for the measurement of the size of microclimate; a portable *Testo 435-2* unit for the measurement and evaluation of the operation of the motor cooling unit, a thermo vision camera and, the dust meter – *Dust Track II 8530*.

4.1.3. Simulations

Supplementary to the experimental testing are numerical simulations. For the purposes of the analysis, a 3D mathematical model for the description of the heat-flow phenomena was developed. The shape and the size of the 3D geometry exactly reproduced the shape and the size of the tested chambers. Using a model of turbulent flows, the researched phenomena were described with the equations of the following: the continuity of flow, movement and energy transportation.

The above differential equations, in their unified, generalized, conservative form, after the isolation of their convection diffusion, and source elements have the form of [9, 10]

$$\frac{\partial(\rho\phi)}{\partial t} + \frac{\partial(\rho u_i \phi)}{\partial x_i} = \frac{\partial}{\partial x_i} \left(\Gamma_\phi \frac{\partial \phi}{\partial x_i} \right) + S_\phi, \quad (1)$$

where: ϕ is a dependent variable, Γ_ϕ is a diffusion transport coefficient, and the source element S_ϕ describes all of the remaining – save convection and diffusion – elements of differential equations; u_i is the velocity vector, x_i is a coordinate, and ρ is the density. Calculations were made using finite volume methods; with the use of *Ansys-Fluent* ver. 13. The results obtained by calculations were verified against the measurements, thus, establishing the usability of the model and providing, at the same time, additional data.

4.2. Test subject

The machine subjected to the test is a 1 MW motor; with a rated voltage and frequency of 6 kV and 50 Hz, respectively; a constant rotary speed of 738 rpm.; a rotor voltage of 1140 V; a rotor current of 560 A; a motor protection level of 44IP; insulation class 130°C (B); a hollow case motor, axial-radial flow airing; calculated cooling air flow of 2.5 m³/s (9000 m³/h). The acceptable ambient temperature for the motor's operation, in accordance with the manufacturer's recommendations, is 40°C. The hollow case motor is Cooley; it is cooled in an axial-radial configuration. The cooling air stream is sucked directly from the precincts of the chamber through openings in the side guards, and directed into the ribs of the motor's frame. It is then directed to the outlets through a channel. On its way out, it partially passes through the winding of the motor's stator and through the spacing between the ribs and the casing. Then, from the inside of the motor, the air is directed into the chamber. The air in the chamber is contaminated with particles of cement dust.

4.3. The PD activity testing and analysis of results

4.3.1. Pre-research

The measurements have been conducted in a continuous manner, with service interruptions from 28 August 2009 until now. Initially, the measurements were taken 3 times a day: at

6:00 a.m., 12:00 p.m., and 6:00 p.m. Then, the frequency of measurements was increased to every 2 hours, and at present, measurements are performed every hour. The data collected during that time is immense. The variability of the partial discharge parameters, during the period in question for one of the phases of motor winding, has been presented in Figure 7.

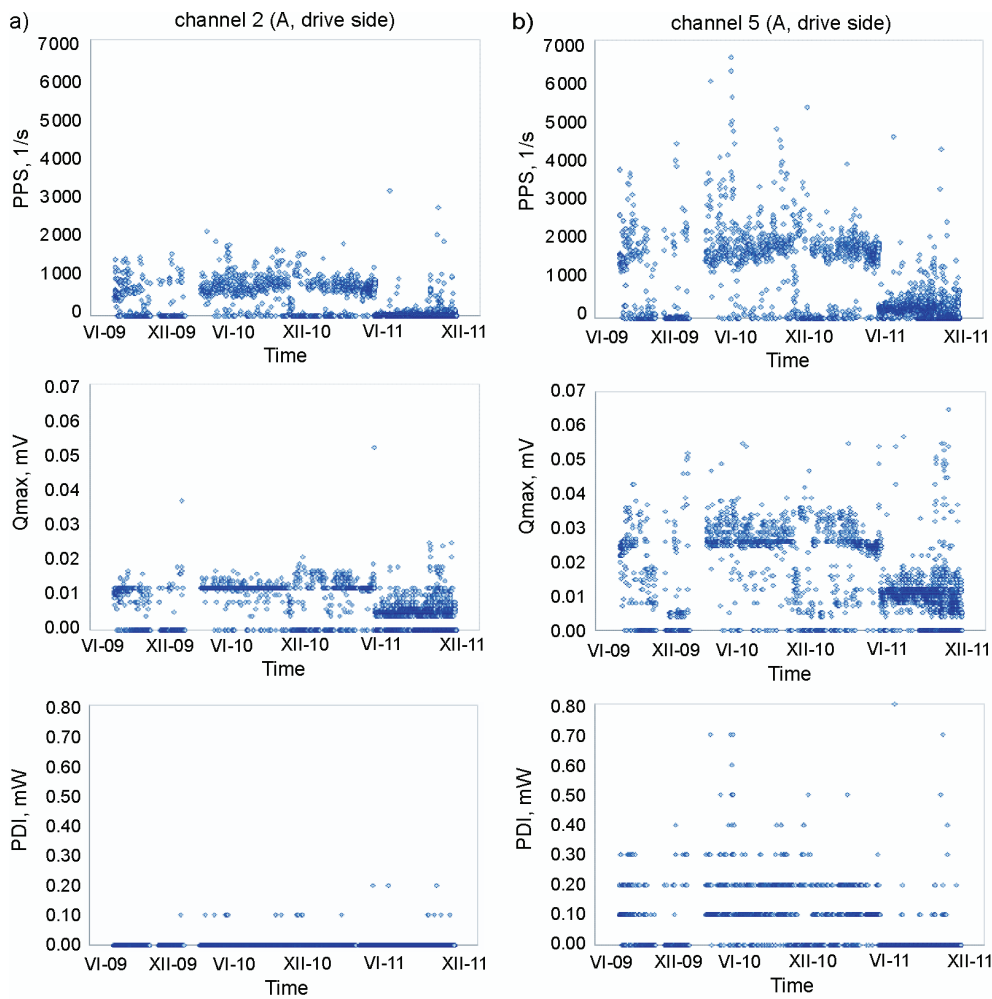


Fig. 7. Histogram of variations of intensity of emission of discharges for a 1 MW motor at PPS, Qmax, PDI: a) channel 2, phase A – drive side, b) channel 5, phase A – non drive side (measurements performed between 28.08.2009 and 31.01.2012)

The frequency of occurring discharges on the drive side and the non-drive side has been presented in Figure 8. The analysis of the accumulated data shows a considerable range of

variation of discharge emission values and that they are temporarily in their character. For comparison sake Figure 9, presents the course of changes in partial discharges for a 9 MW induction motor. Here, the variability of parameters points to temporary changeability of the *PD* intensity and the advancing ageing process presenting itself in the form of an increased magnitude of *PD* changes.

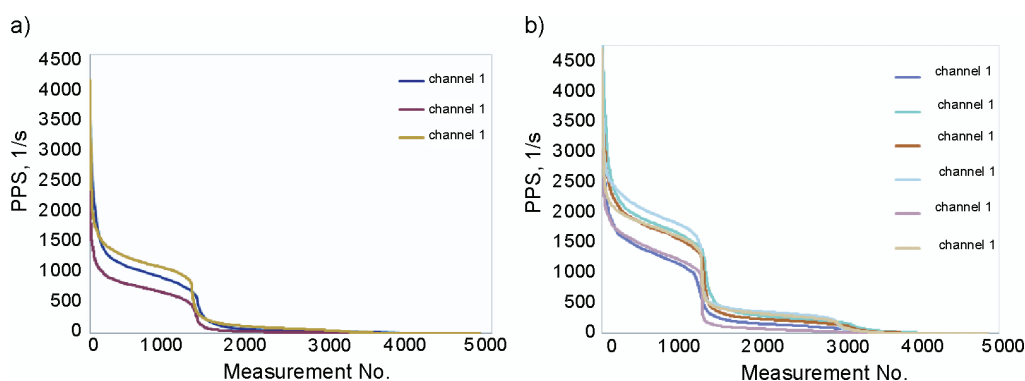


Fig. 8. The frequency of occurring discharges a) the drive side b) the non-drive side; (measurements performed between 28.08.2009 and 31.01.2012)

It is appropriate, from the point of view of the analysis of the influence of individual values of the emission of partial discharges, to analyze the individual motor operation cycles in varying operating conditions and in varying ambient conditions. Figure 10 presents the range of *PD* activity during one cycle of the motor's operation in summer and in winter conditions, and also presents mutual correlation of temperature, humidity, load and moisture content in the air, the magnitude (Q_{max}) and the intensity of partial discharge (*PPS*, *PDI*). The analysis shows that a negative correlation between temperature increase and the amplitude of discharges can be observed (correlation coefficient of 0.80–0.90). However, inverse tendency, and an increase in the number of discharges can be observed after the temperature rises above 35°C.

During the motor's operation in winter conditions, a rise in air temperature in the range of 0÷20°C causes increases in *PD* magnitude (positive correlation).

An analysis of the results gave rise to a number of questions whose answering requires additional detailed testing. For example, clarification was required concerning the character of influence of changes in humidity and temperature on the *PD* activity. During the regular operation of the motor, the system recorded sudden changes in *PD* activity. As it turned out in the course of detailed analysis, the reason was found in the employees' opening the door of a chamber in which the motor is located. It is a complex problem especially that individual mutual correlation coefficients, which are recorded during the measurements, decide on the results of the diagnosis within the scope of evaluating the insulation condition. Another problem that needed to be solved was the establishment of the frequency of *PD* measurements,

time sequence conditions, and whether the room was properly adapted for operating machines, and if and how microclimatic conditions in the room affected the results of the measurements. All of those factors turn out to be immensely crucial from the point of diagnostic evaluation. That is why a detailed analysis of the selected microclimatic values on *PD* emissions had to be conducted.

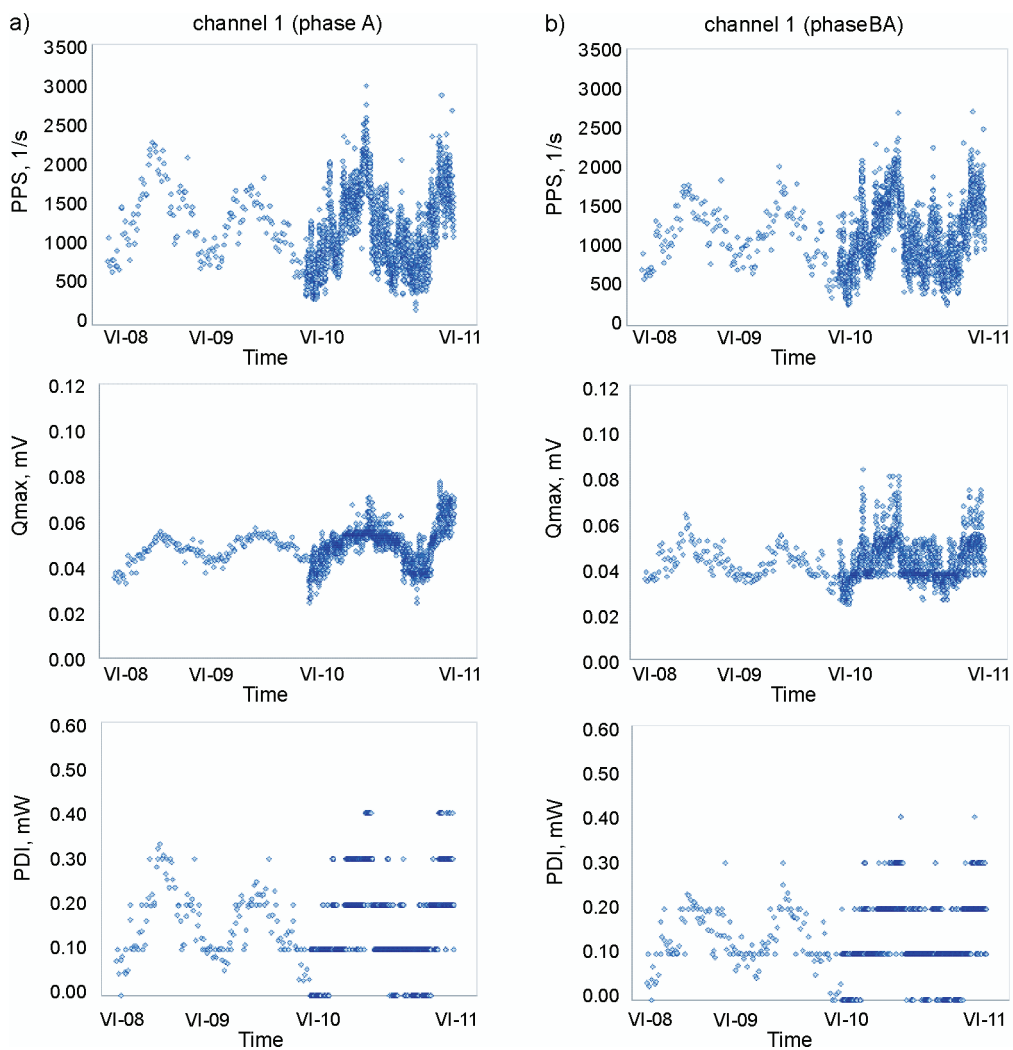


Fig. 9. Histogram of variations of intensity of discharge emissions for a 9 MW motor: PPS, Qmax, PDI: a) channel 1 – phase A, b) channel 2 – phase B; Measurements performed between 01.06.2008 and 31.01.2012

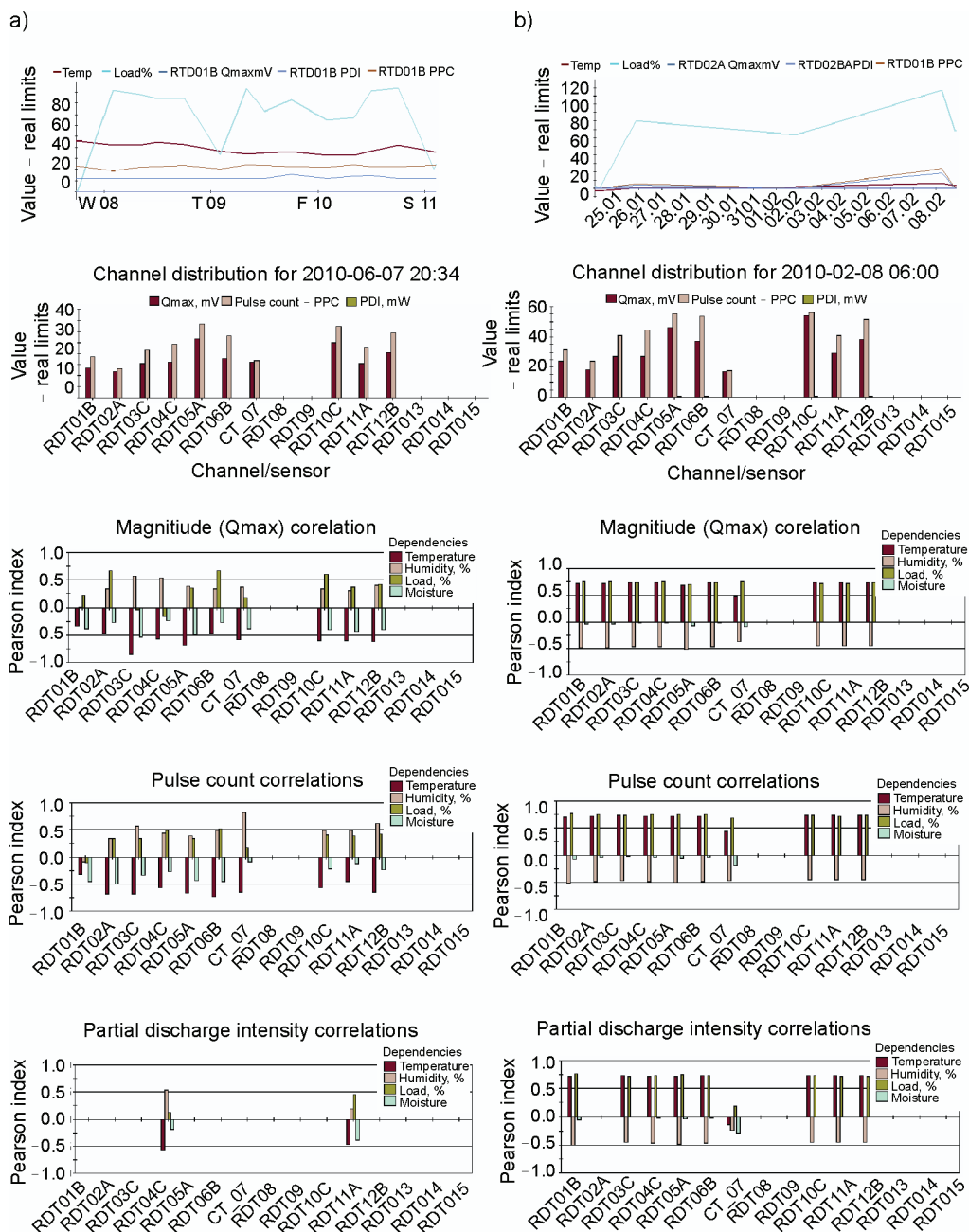


Fig. 10. Analysis of the effect of motor load and environmental conditions (temperature, relative humidity, air humidity contents) on PD emission in a) summer conditions (1-3.06.2010) b) winter conditions (01-03.06.2010).

4.3.2. Analysis of thermal and air flow conditions in the room

The motor research is performed on a temporary basis, which directly affects microclimatic conditions in the room. With no heating system present, the heat flux gains from the working motor and the auxiliary equipment are the main sources of heat in the room. In the course of measurement using a thermo vision camera, it turned out that apart from the motor, the mechanical transmission is also an intensive heat source. On its surface, the temperature remains in the range 35-55°C. Depending on the season of the year (Fig. 11), the mentioned sources transfer the heat by means of radiation and convection. The effect the operating motor has on the temperature in the room, has been presented in Figure 12. The following conclusion is that at loads of 70-100%, heat exchange by convection equals to 45-40 kW (Fig. 12b). The result is that with a simultaneous operation of both motors, the rise in air temperature in the room often exceeds 45°C (Fig. 12a). The temperature of airstream temperature passing through the motor rises along with the room temperature. Within a room temperature range of 0-20°C, it rises on average by 10°C (Fig. 12b).

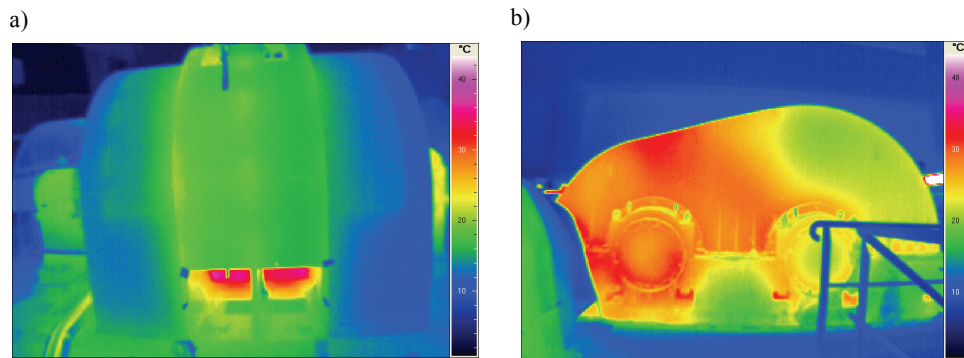


Fig. 11. Temperature distribution on: a) the operating motors in a room having an average temperature of 10°C b) the surface of the transmission, measurement conditions same as above

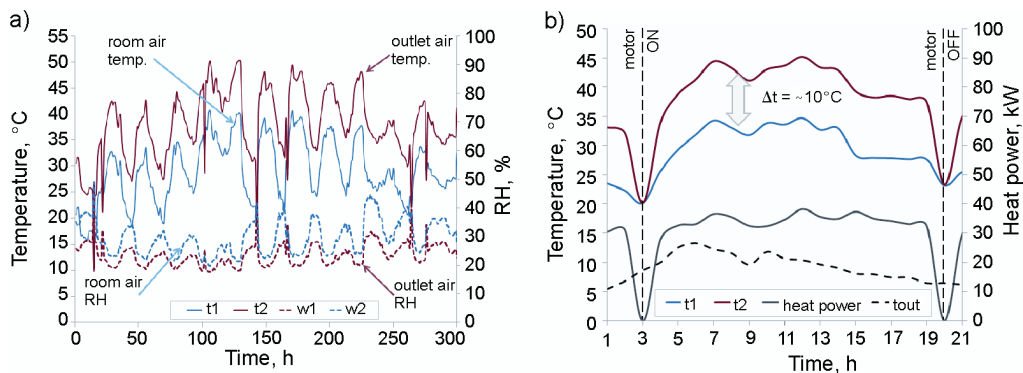


Fig. 12. The influence of the operating motor on a) the parameters of the surroundings in which the researched motor operates b) the emission of air into the surroundings

The results of the calculations verify the measurements, and at the same time, they supply a number of additional information (Fig. 13). The colour scale corresponds to temperature. The research also shows that the operating motors cause much heterogeneity of the field of temperature and velocity. At an external temperature of 0°C, the irregularity reaches 26°C. At a velocity range of 0.3-9 m/s, the convection mechanism sets air particles into motion in the entire room, and thus causes spatial circulation. As a result of that, the SE-1 motor, during the axial intake of the air from the side of the transmission and from the side of the room, does not have ensured the cooling symmetry. Differences in temperature may reach 10°C in the summertime.

The reason for the asymmetrical cooling of the motors may also lie in the disturbances of free air flow. In the researched system, one of the safety shields was mounted too close to the spinning part of the shaft at the non-drive side which caused restrictions on the access of air flow. As a result, the restrictions reached 20%. In consequence, this part of winding transfers 5 kW of heat less into the environment, which causes a local increase in the temperature of winding to a level of 20°C. An imbalanced cooling of the motor winding also leads to an increase in local partial discharges. The influence of the air temperature on the quantity of partial discharges at both sides of the cooling system (drive side and non-drive side), phase A, has been presented in Figure 14. It can clearly be seen that the operation of winding in worse-cooled areas promotes an increased number of discharges (*PPS*) and an increase in their intensity (*PDI*).

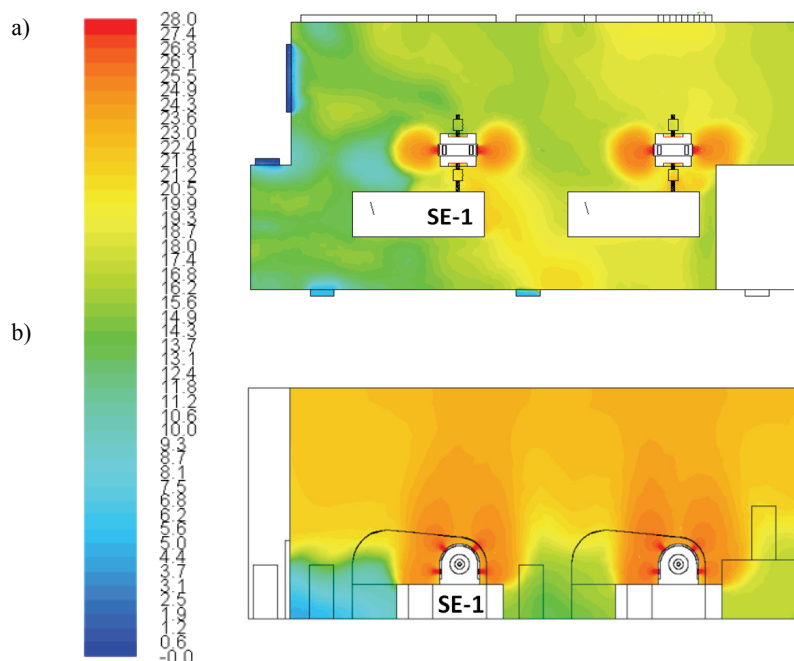


Fig. 13. Distribution of the air in horizontal temperature a) on a horizontal plane b) on a vertical plane, in the engine room

4.3.3. Analysis of the microclimate on PD emissions

The correlation between the external environment parameters and values describing the activity of PD, established by way of a large measurement group (4 000 measurements), has been presented in Figures 14-16.

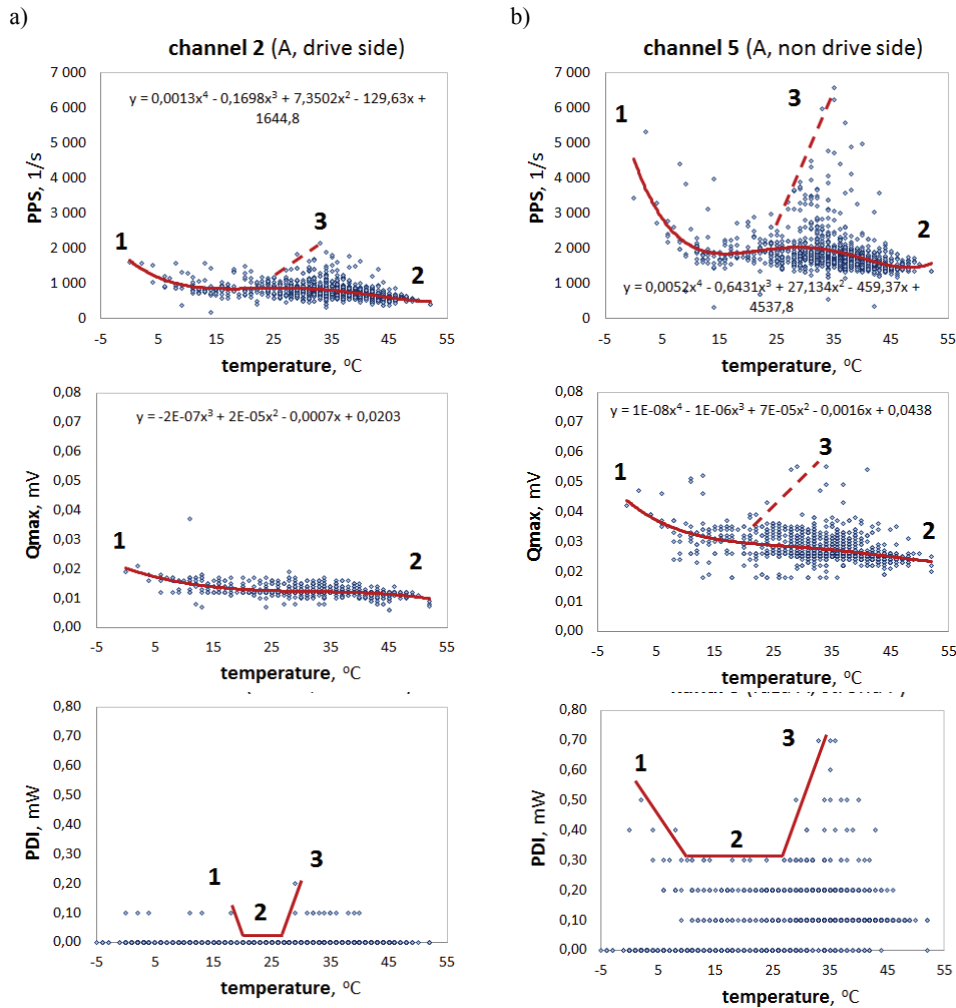


Fig. 14. The impact of air temperature on the emission PPS, Q_{max} and PDI: a) channel 2 – drive side, b) channel 5 – non drive side (measurements performed between 28.08.2009 - 04.07.2011)

The distribution of the intensity of discharges (PPS) in the function of the air temperature shows that when the temperature is lower than 10°C, a clear increase in the intensity of discharges occurs (Fig. 14 – line 1). When the temperature of the air increases, the trend line drawn by the linear approximation shows drops in the number of discharges (Fig. 14 – line 2). However, measurements within this range show that there are moments when the intensity of

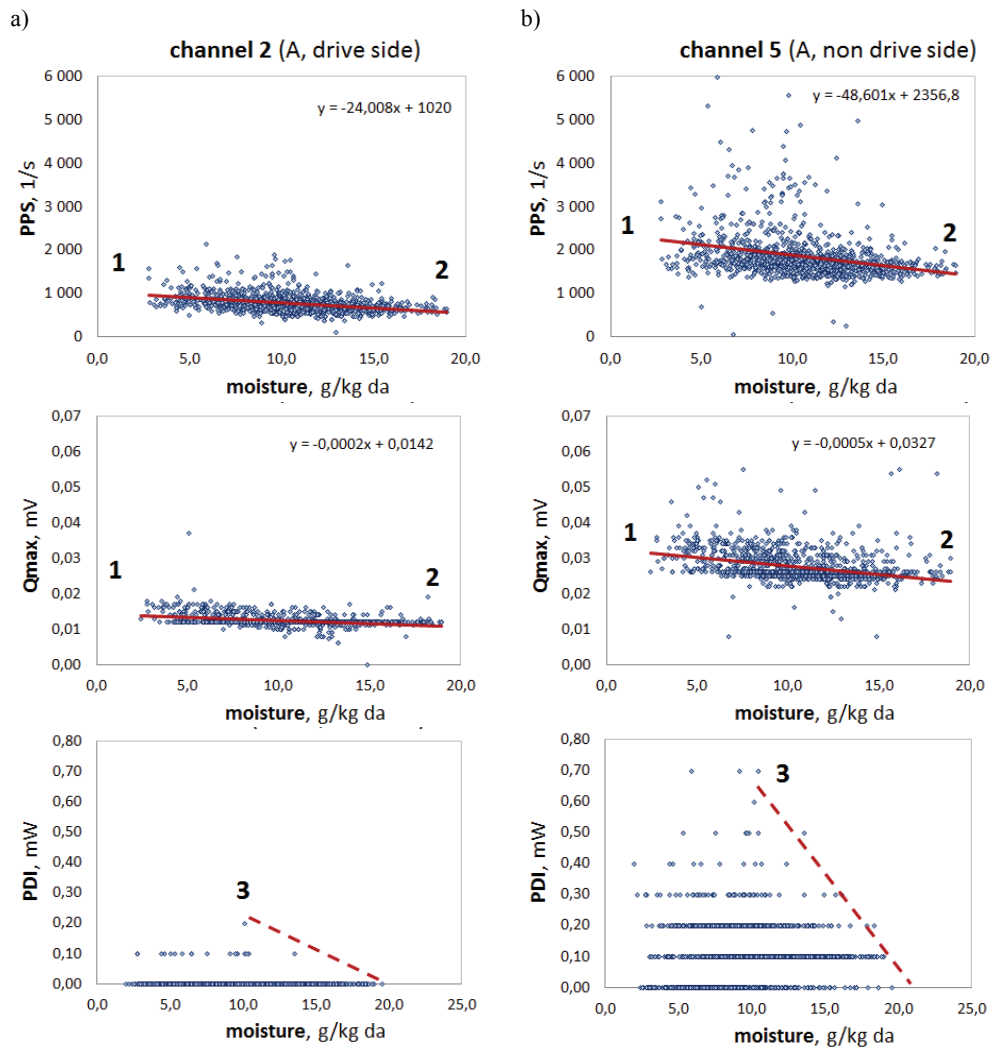


Fig. 15. The impact of the moisture of the air on the PPS , Q_{max} and PDI : a) channel 2 – drive side, b) channel 5 – non drive side (measurements performed between 28.08.2009 - 04.07.2011)

discharges rises as much as 2.5 times in relation to the number of impulses picked up at the temperature range of 10-30°C. This increase can be clearly observed at the increase in temperature to the range between 20-35°C (Fig. 14 – line 3). The change of the Q_{max} parameter, as the function of the temperature of the air, has been presented in Figure 14. The value of this parameter corresponds to the magnitude of 10 picked up discharges recorded within 1 second. This graph also shows that below a temperature of 10°C, a clear increase in the Q_{max} parameter occurs (Fig. 14 – line 1). The increase in temperature affects the reduction of the discharge magnitude (line 2). In this graph, one can observe two levels of discharges (lines 2 and 3). Both lines have a similar directional coefficient, which verifies the observed tendency. Both

magnitude levels observed confirm the impact of the level of dusting of the air with cement dust on magnitude Q_{max} . Very interesting inferences can be drawn from the observation of the influence of air temperature on the value of discharges (PDI) (Fig. 14). Lines 1, 2, and 3 show the area in which the value of discharges is at its lowest. Within the range of 10-25°C, the discharges do not exceed 0.3 mW. A fall or increase in temperature in this range clearly shows a decrease in discharge, even by 50%. The influence of humidity on the air on the activity of discharges has been presented in Figures 15 and 16. Air humidity has been presented in these figures by value – expressing the content of moisture in dry air, and in percent – relating to relative humidity.

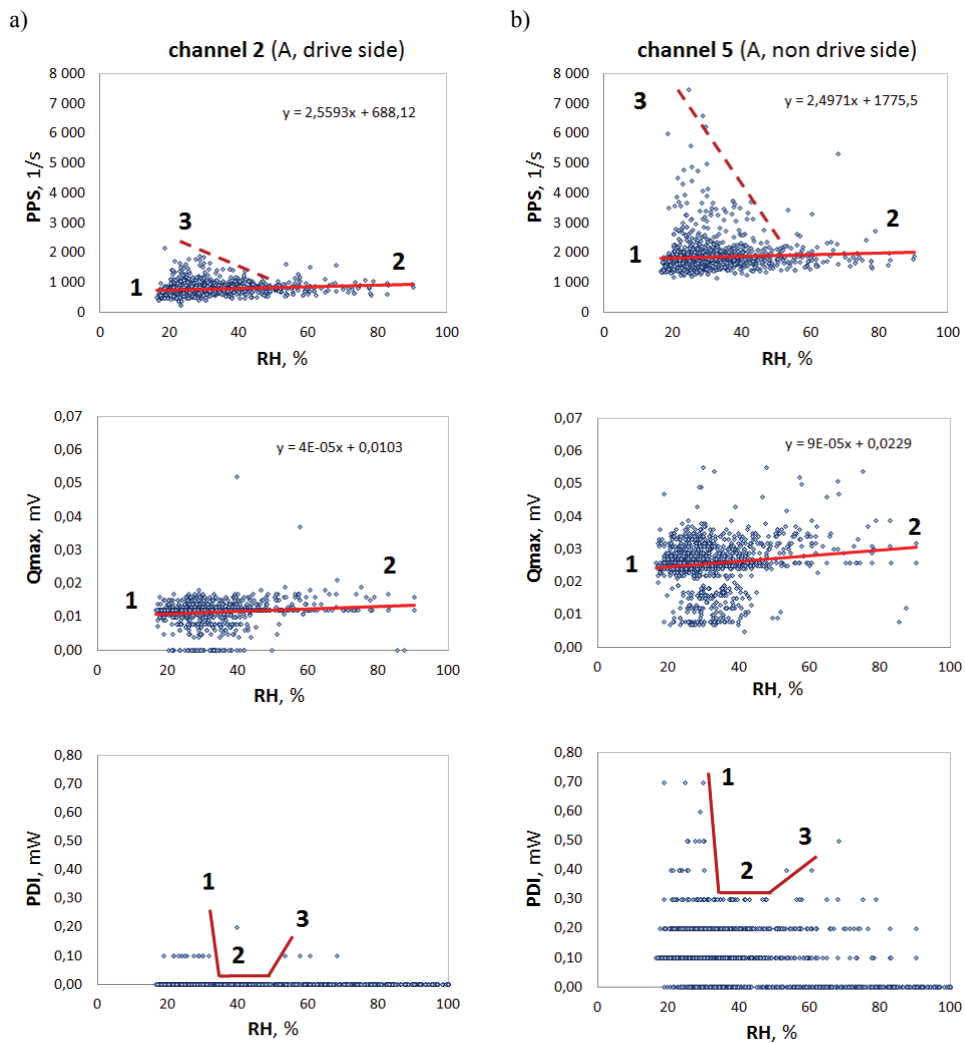


Fig. 16. The impact of relative humidity of the air (RH) on the PPS, Q_{max} and PDI: a) channel 2 – drive side, b) channel 5 – non drive side (measurements performed between 28.08.2009 - 04.07.2011)

By expressing PD as a function of the humidity of the air, one can draw the inference that intensity, magnitude, as well as the pulse count rate is lower together with the increase in humidity. This proves that along with an increase in humidity, heat capacity of the air increases, which improves the intensity of heat exchange between the stator's and rotor's winding, and the cooling airstream flow (better cooling effectiveness). Slightly different conclusions can be reached when the activity of discharges in the function of relative humidity is expressed. Activity of discharges is very intensive when relative humidity drops below 30% (line 1). But also an increase in relative humidity causes an increase in discharges (lines 1 and 3).

The analysis that has been presented thus far, considered the influence of temperature and air humidity on the activity of discharges, separately. The state of any single-component gas is described explicitly in terms of temperature when two of its parameters are known, for example pressure and temperature. A third parameter can be calculated with the equation of state. However, to establish the thermal state of humid air, which is a mix of two gases, one requires additional knowledge of the air make-up, for example water vapour content X . As an auxiliary tool for the answering of questions occurring in practice and especially for the calculation of balances of processes, graphs of humid air can be used. The most commonly known are the *Mollier* graphs that describe the state of the air in coordinates $h-X$ (h – enthalpy, X – water vapour content), and the *Carrier* graphs in coordinates $t-X$ (t – temperature). In these graphs, the remaining parameters, for example relative humidity φ , are represented as parametric family lines. Figure 17 presents a set of points that describe thermodynamic states of humid air that correspond to the measurements performed in the immediate surroundings of the motor subjected to research that have been presented as coordinates in accordance with the Carrier graph. Measurement points have been grouped in accordance with their PDI and Q_{max} coefficient, thanks to which the arrangement corresponding to the lowest and the highest values of discharge activities were obtained. The conducted analysis shows that the optimal ambient conditions, at which the PD emission is the lowest, are contained within the range of: temperatures $t = 25-45^{\circ}\text{C}$, relative air humidity $\varphi = 18-50\%$ and water vapour content $X = 8-17$ g/kg of dry air.

5. Conclusions

The subject matter presented in the article involves problems in the area of diagnostics of HV electric machines and the analysis of thermal and air flow phenomena that accompany the operation of these machines, as well as the evaluation of their impact on the quantity of PD emission. The ageing process, in the insulation of electric motors, is not fully explained. The most important matter when continuously monitoring the condition of insulation of motors, is the continuous scrutiny of the tendency of changes in the measured quantities and features, especially: PPS , Q_m (Q_{max}), PDI , or the Phase Resolved PD Patterns. Defining the alarm level values should be performed in relation to one's own database or that of the manufacturer of the diagnostic equipment. If a sudden increase in the measured values is observed, for example, a 2.3 times increase over the period of a month, the motor should be brought to

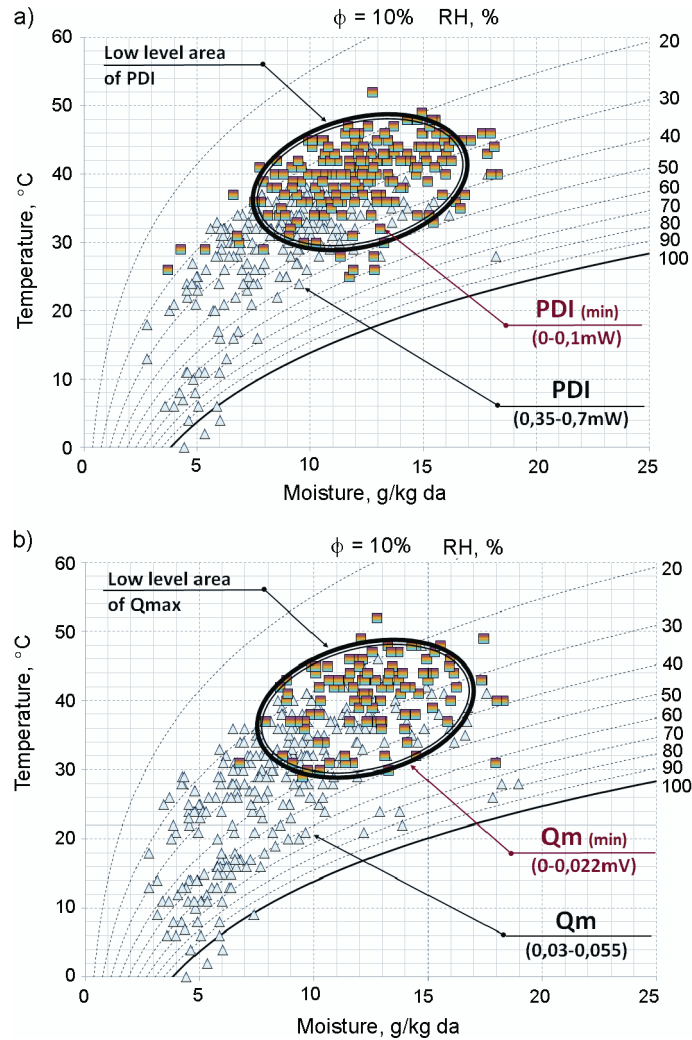


Fig. 17. PD activity in the psychrometric Carrier graph, a) PDI , b) Q_{max} (Q_m); phase A, channel 5 (measurement from 28.08.2009 to 04.07.2011)

a standstill. In such a case, a thorough inspection connected with maintenance servicing activities, or even refurbishment, is required. Startup of the motor should be examined by means of measurements of the condition of insulation in adherence to off-line methods. The data accumulated in the course of the tests also supply a number of supplementary information. They clearly show that there is no indirect influence of ambient elements on PD emission. It has been demonstrated in the example of one of the tested motors that it is possible pinpoint the most favourable microclimatic conditions in which the PD intensity is the lowest. It should be therefore concluded that it is crucial for the HV motor room that microclimatic conditions are controlled, thus bringing PD activity to a minimum. The comparison of partial discharge of the motor operating in variable ambient conditions, with prognosed activity, when the

ambient conditions are formed in accordance with a specific area, has been presented in figure 18. It shows that considerable PD reduction should be expected by controlling temperature and humidity in the motor room, thus prolonging the motor's lifetime. Maintenance of the required ambient conditions in the operating rooms is possible only when we have an appropriate thermal ventilation system at our disposal. Such a system should be designed taking into account the geometry of the room, its location, and the interaction of the most important elements, from the point of view of heat exchange and the mass of the motor. For that purpose, for example, modern methods of phenomena simulation should be applied. The ventilation system should work in a continuous manner, thus regulating temperature and humidity in accordance with a given algorithm.

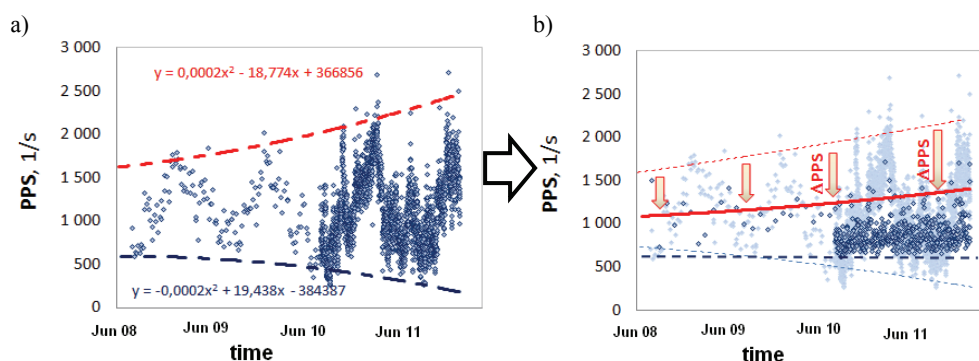


Fig. 18. Prognosed PD emission reduction as a result of the maintenance of conditions of thermal comfort, showing a) PD emission without regulated environmental parameters b) PD emission with regulated environmental parameters

References

- [1] ADWEL, *PD monitoring*. Nota Aplikac. (2003).
- [2] Bendat J., Piersol A., *Metody analizy i pomiaru sygnałów losowych*. Państwowe Wydawnictwo Naukowe, Warszawa (1976).
- [3] Bertenshaw D., Sasic M., *On-line Partial Discharge Monitoring on MV motors-Casestudies on Improved Sensitivity Couplers*. Nota Aplikacyjna firmy ADWEL International Canada (2002).
- [4] Bruetsch R., Tari M., Isola R. et al., *High Voltage Insulation Failure Mechanisms*. IEEE International Symposium on Electrical Insulation, Vancouver, BC Canada, June 8-11 (2008).
- [5] Dąbrowski M., *Projektowanie maszyn elektrycznych prądu przemiennego*. WNT, Warszawa (1994).
- [6] Blokhintsev D., Golovkov M., Golubev A., Kane C., *Field Experiences on the Measurement of Partial Discharges on Rotating Equipment*. IEEE PES'98, February 1-5, Tampa (1998).
- [7] Kabza Z., Lichota J., Plutecki Z., *Pomiary energetyczne dla potrzeb wyboru optymalnych warunków użytkowania budynków „zrównoważonego rozwoju”*. Raport końcowy do projektu badawczego PB Nr 8 T10C 006 19, Praca niepublikowana, Opole (2003).
- [8] Plutecki Z., *Wieloparametryczna ocena warunków komfortu cieplnego*. PAK 02: 153-156 (2011).
- [9] Plutecki Z., *Analiza zjawisk ciepłno-przepływowych w ogrzewanym pomieszczeniu*. Archiwum Energetyki XXXIII(1-2), Wydawnictwo Komitetu Problemów Energetyki przy Prezydium PAN, Gdańsk (2004).

- [10] Plutecki Z., *Analiza wpływu mikroklimatu na emisję wyladowań niezupełnych w maszynach elektrycznych. Studia i Monografie*. z. 325. Oficyna Wydawnicza Politechniki Opolskiej, Opole (2012).
- [11] Stone G.C., Boulter E.A., Culbert I., Dhirani H., *Electrical insulation for rotating machines*. IEEE PRESS series on Power Engineering, USA (2004).
- [12] Szymaniec S.: *Diagnostyka stanu izolacji uzwojeń i stanu łożysk silników indukcyjnych klatkowych w warunkach przemysłowej eksploatacji*. Studia i Monografie z. 193, Wydawnictwo Politechniki Opolskiej, Opole (2006).
- [13] Szymaniec S.: *Wykorzystanie funkcji korelacji w pomiarach on-line wyladowań niezupełnych silników elektrycznych w przemyśle i energetyce*. Energetyka 10: 675-680 (2010).
- [14] Younsi K., Snopek D., Hayward J. et al., *Benefits of partial discharge analysis - Seasonal Changes in Partial Discharge Activity on Hydraulic Generators*. Estudios-Elctricos 2E News 7: 07-11 (2010).
- [15] Stone G.C., Lloyd B., Sasic M., *Experience With Continuous On-Line Partial Discharge Monitoring of Generators and Motors*. 2008 International Conference on Condition Monitoring and Diagnosis, Beijing, China, April 21-24 (2008).
- [16] Lloyd B., Campbell S.R., Stone G.C., *Continuous On-Line Partial Discharge Monitoring of Generator Stator Windings*. IEEE Transactions on Energy Conversions pp. 1131-1137 (1999).
- [17] Younsi K. et al., *Seasonal Changes in Partial Discharge Activity on Hydraulic Generators*. Proceedings of Electrical Insulation Conference and Electrical Manufacturing & Coil Winding Conference (2001).